

Measurement of Reactive Power in Single-Phase Networks by Use of the Walsh Functions

Adalet Abiyev, *Member, IEEE*

Department of Electrical and Electronics Engineering, Girne American University, P.O. Box:5, Karaoglanoglu, Kyrenia, North Cyprus, Mersin-10, Turkey, aabiyev@gau.edu.tr

Abstract—This paper describes Walsh function (WF) based method for the evaluation of reactive power (RP) component from instantaneous power signal in the sinusoidal conditions. Proposed method simplifies the multiplication procedure to evaluate the reactive components from instantaneous power signal. The advantages of the proposed method have been verified by experimental studies. One of these advantages is that in contrast to the known existing methods which involve phase shift operation of the input signal, the proposed technique does not require the time delay of the current signal to the $\pi/2$ with respect to the voltage signal. Another advantage is related to the computational saving properties of the proposed approach coming from use of the Walsh Transform (WT) based signal processing method. Validity and effectiveness of the suggested method for evaluation of the RP components of the electrical power have been tested by use of a simulation tool developed on the base of “Matlab”.

Keywords—Signal processing, DSP, Walsh function, reactive power evaluation, instantaneous power signal, phase shift.

I. INTRODUCTION

The strong requirements to the efficiently transmission, distribution, and consumption of electrical energy have always been and remain as actual problem. Evidently the RP is the one that sufficiently influences to the efficiency of power system operation. The RP overloads the transmission line and negatively affects the stable operation of power systems [1]. One of the key approaches for solution of this problem is the proper selection of the RP compensating method and corresponding devices but latter mostly depends on the knowledge about the portion of reactive component in the total power. That is why an accurate measurement of RP is extremely important task in power systems operation and control.

Through the recent decades various RP evaluation approaches have been investigated and developed for application in sinusoidal as well as in harmonically distorted single- and three-phase power systems. An application of wavelet transform involving phase shifting operation for measuring RP was developed in

[2]. Use of frequency insensitive quadrature phase shifting approach to the measurement of reactive power is described in [3], where a time-division multiplier type wattmeter is used to achieve the final results. In [4] a stochastic signal processing method was investigated and applied for realization of a reactive power and energy meter. Different types of the calculation algorithms, such as a computer algorithm [5], the artificial neural networks [6], the digital infinite impulse response filtering [7], and the least error squares estimation algorithm [8], have been applied for evaluation of RP in power systems.

Although the Fourier transform (FT) based digital or analogue filtering algorithms allow the evaluation of RP without shifting operation but a large number of multiplication and addition operations are required when applying FT algorithms for RP evaluation. For example for a 16 point DFT $16^2 = 256$ complex multiplications and $16 \times 15 = 240$ complex addition operations are required. The various algorithms (for example FFT known as the Cooley Tukay algorithm) have been developed to reduce the number of multiplication and addition operations by use of the computational redundancy inherent in the DFT.

Unfortunately, FT based algorithms are still computationally complex.

The attraction of WF based approach to RP evaluation comes from the key advantages such as following:

(a) a requirement of IEEE/IEC definition of a phase shift of $\pi/2$ between the voltage and the current signals, typical for reactive power evaluation [3] is eliminated from signal processing operation;

(b) the multiplication operation between two digital data is replaced with the multiplication operation between digital data and positive or negative unit (+1 or -1). In other words, the multiplication operation is performed by simple altering the sign of the given digital data from positive to the negative sign so that to be multiplied by -1. Thus the WT analyzes signals into rectangular waveforms rather than sinusoidal ones and is computed more rapidly than, for example FFT [9]. WT based algorithm contains

additions and subtractions only and as a result considerably simplifies the hardware implementation of RP evaluation.

The authors in [10] have analyzed WT algorithms employed to energy measurement process and they have shown that the Walsh method represents its intrinsic high-level accuracy due to coefficient characteristics in energy staircase representation. Authors in [11] states that decimation algorithm based on fast WT(FWT) has better performance due to the elimination of multiplication operation and low or comparable hardware complexity because of the FWT transform kernel.

The new 2-Dimensional digital FIR filtering based algorithms for measuring of the RP are proposed in [12]. Ibid the WF based existing RP measurement algorithm is cited. The basic idea of this WF based algorithm consists in the resolving of the voltage and current signals separately along the WFs, at first, and then obtaining the RP as the difference of the products of the quadrature components. At least four multiplication-integration, two multiplication, and one summation operations required for RP evaluation makes this algorithm comparatively complex and less convenient for implementation.

It was the aim of this paper to evaluate RP component from instantaneous power signal without phase shift of $\pi/2$ between the voltage and the current waveforms with relatively less computational demands. This objective was achieved by using the WF.

The paper is organized as follows. In section two the WF based analogue and digital signal processing approaches for RP evaluation are described. The DSP based evaluation approach by using discrete is proposed in section three. In section four the simulation results of WF based RP evaluation system are given. Section five includes the conclusion of the paper.

The classic way to determine the reactive power includes evaluation of the reactive power by using the measured values of the apparent power S , and the active power P . They are defined as:

$$S = UI, \quad P = UI \cos(\varphi)$$

Having the apparent power S and the active power P , the reactive power Q is determined as

$$Q^2 = S^2 - P^2 \quad \text{or} \quad Q = UI \sin(\varphi).$$

This way of RP evaluation confirms the necessity of measuring of the root mean square (RMS) values of voltage U and current I , and then performing the multiplication operation in order to obtain apparent power S . But this operation is complex due to the

measuring of the RMS values of U and I , which are difficult to measure.

II. AN ANALOG AND DIGITAL SIGNAL PROCESSING ALGORITHMS TO RP EVALUATION

A. Analogue Measurement Algorithm

Assume that in single-phase circuit a source voltage $u(t)$ and a current flowing through load $i(t)$ are the pure sinusoidal signals. Then the instant power $p(t)$ is given by [5],[8]

$$p(t) = P - [P \cos 2\omega t + Q \sin 2\omega t] \quad (1)$$

Time diagram representation of the right-hand side terms of (1) is shown in the Fig.1. Fig.2 represents the third order WF, $Wal(3,t)$ with the normalized period of $T/2$ [9].

Multiplication of both sides of (1) by the third order WF, $Wal(3,t)$ is given by

$$p(t)Wal(t) = PWal(3,t) - P \cos 2\omega t Wal(3,t) - Q \sin 2\omega t Wal(3,t) \quad (2)$$

Time diagram representation of the right-hand side terms of (2) is shown in the Fig.3. It is important to note that multiplication of (1) by the $Wal(3,t)$ results in rectification of reactive component of the power, $p(t)$ (Fig.3, curve 1).

In the next step we take integral from both sides of (2) during time period of T (2):

$$\frac{1}{T} \int_0^T p(t) \cdot Wal(3,t) dt = \frac{1}{T} \int_0^T P Wal(3,t) dt - \frac{1}{T} \int_0^T P \cos 2\omega t \cdot Wal(3,t) dt - \frac{1}{T} \int_0^T Q \sin 2\omega t \cdot Wal(3,t) dt \quad (3)$$

As can be seen from Fig.3 the average value of both product functions of $PWal(3,t)$ and of $P \cos 2\omega t \cdot Wal(3,t)$ during the time period T equal to zero. Thus, the first and second integrals in the right-hand side of (3) become zero. Thereby (3) is rewritten as follows

$$\frac{1}{T} \int_0^T p(t) \cdot Wal(3,t) dt = \frac{1}{T} \int_0^T Q \sin 2\omega t \cdot Wal(3,t) dt \quad (4)$$

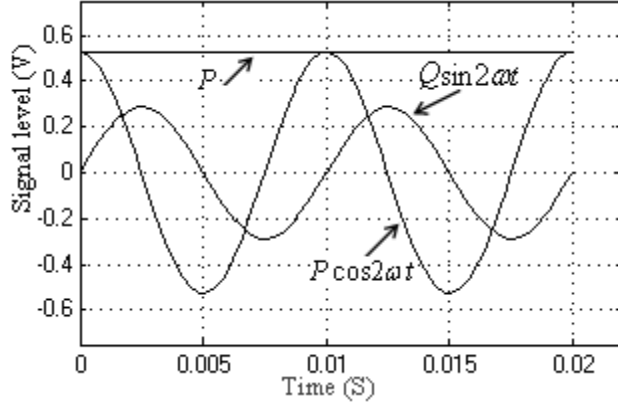


Fig.1. Graphical interpretation of the power components defined by (1).

$$\omega = 2\pi/T, T = 1/f, f = 50\text{Hz}, u(t) = 2.4\sin\omega t$$

$$i(t) = 0.5\sin(\omega t - 0.5)$$

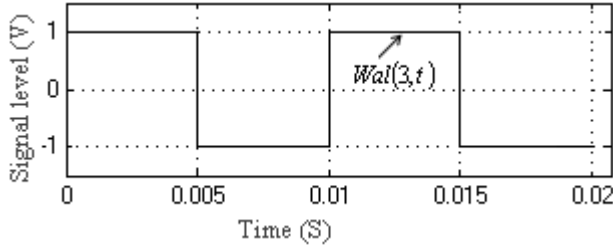


Fig.2. Graphical interpretation of third order Walsh function.

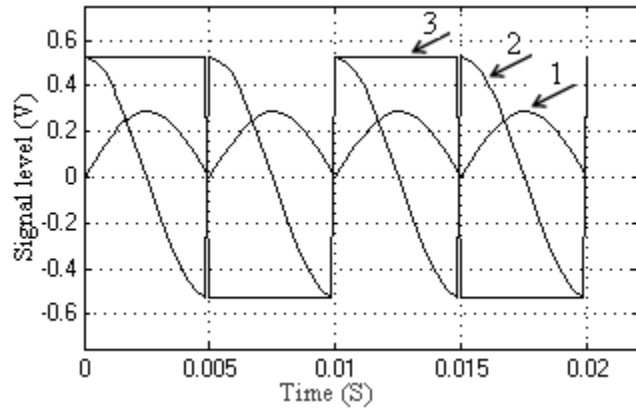


Fig.3. Graphical interpretation of third order Walsh function
1- $Q\sin 2\omega t \cdot Wal(3,t)$; 2- $P\cos 2\omega t \cdot Wal(3,t)$; 3- $PWal(3,t)$

Carefully look at the curve 1(Fig.3) and the integral given by (4) allow us to summarize that the average value of the oscillating reactive power can be measured by use of the derived algorithm without the phase-shift operation of the voltage(or current) signal to the $\pi/2$ with respect to the current(or voltage)signal.

Mathematical expression for RP evaluation is obtained from (4) considering Fig.3 (curve 1), as follows

$$Q = \frac{1}{T} \int_0^T p(t) \cdot Wal(3,t) dt = \frac{1}{T} \int_0^T |Q\sin 2\omega t| dt \quad (5)$$

As a result integral of equation (8) gives average value of the reactive power.

B. Digital Measurement Algorithm

To derive the digital measurement algorithm for RP an expression for instantaneous power given by (1) can be rewritten in discrete form as follows

$$p(n) = P \left[P \cos\left(\frac{4\pi}{N} \cdot n\right) + Q \sin\left(\frac{4\pi}{N} \cdot n\right) \right] \quad (6)$$

Where $n = 0, 1, 2, \dots, N-1$. N is the number of samples in power of 2. N is determined in accordance with sampling theorem[9]: $N = T/T_s$, T_s is the sampling period.

For derivation of the digital algorithm for the RP evaluation we use the discrete expression of the WF [13]-[15]:

$$Wal(i, \beta_k) = (-1)^{\sum_{k=1}^m (\omega_{m-k+1} \oplus \omega_{m-k}) \beta_k} \quad (7)$$

where i is order of WF in the WF system, $i = 0, 1, 2, \dots, N-1$, β_k is argument of WF and defines the bit(digit) coefficients of β_k represented in binary code, $\beta = (\beta_1, \beta_2, \dots, \beta_k)_2$, $\beta_k = 0, 1$, ω_m is the bit(digit) coefficients of ω_m represented in binary code, $\omega = (\omega_0, \omega_1, \omega_2, \dots, \omega_m)_2$, $\omega_m = 0, 1$, m is a binary representation of highest-order WF serial number in the WF system. For evaluation of the reactive component of EP we use the third-order WF, $Wal(3, \beta_k)$. For the third-order Walsh function $\omega = 3$ therefore only $\omega_6 = 1$ and $\omega_5 = 1$. Remaining bit coefficients of the ω_m , $m = 1, 2, 3, 4$ are equal to the zero: $3 = (000001)_2$. In this case the third-order WF is given by

$$Wal(3, \beta_2) = (-1)^{(\omega_5 \oplus \omega_4) \beta_2} = (-1)^{(1 \oplus 0) \beta_2} = (-1)^{\beta_2} \quad (8)$$

The argument, β_k changes depending on normalized time of $T = 0.02\text{sec}$. as shown in the Fig.4. Fig.5 depict the β_2 and third-order discrete WF.

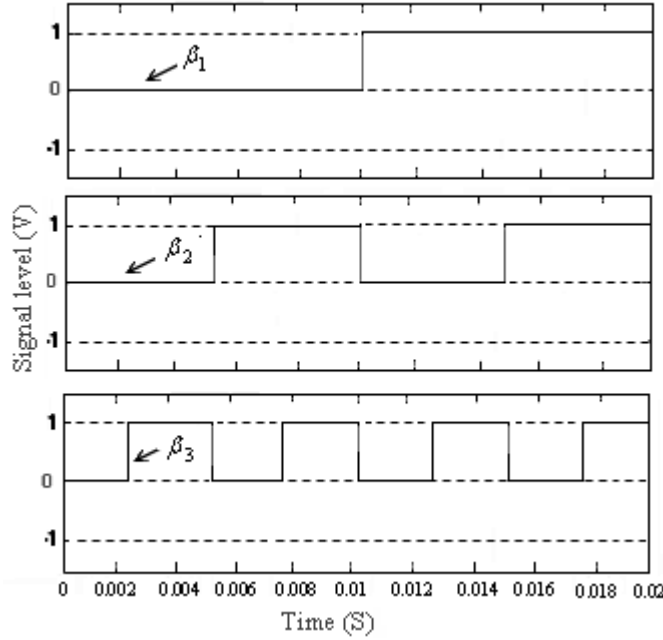


Fig.4. Time representation of final three bit coefficients of the binary representation of β_k

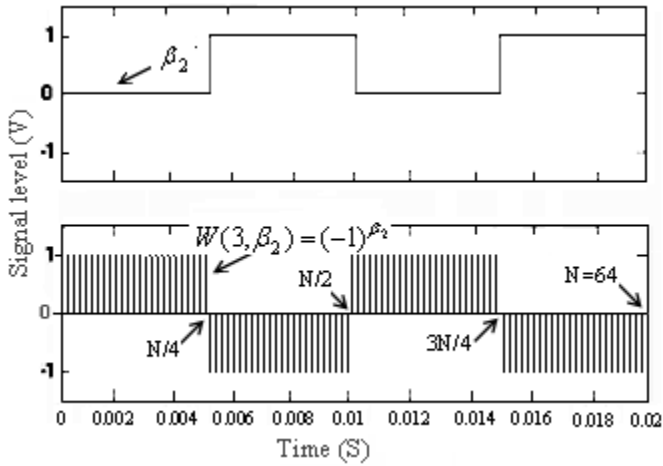


Fig.5. Time representation of β_2 and third-order discrete WF

To achieve the stated in the introduction objective we multiply both sides of (4) by (7) and sum the product terms over the $n = 0, 1, 2, \dots, N-1$, that is

$$\frac{1}{N} \sum_{n=0}^{N-1} p(n)(-1)^{\beta_2} = \frac{1}{N} \sum_{n=0}^{N-1} P(-1)^{\beta_2} - \sum_{n=0}^{N-1} P \cos(4\pi n/N)(-1)^{\beta_2} - \sum_{n=0}^{N-1} Q \sin(4\pi n/N)(-1)^{\beta_2} \quad (9)$$

As a result of the fact that the $(-1)^{\beta_2}$ is periodic and $\cos(4\pi n/N)$ is orthogonal with the $(-1)^{\beta_2}$ over the $n = 0, 1, 2, \dots, N-1$, the first and second terms on the right side of (12) are zero. Thereby, the (12) is given by

$$\frac{1}{N} \sum_{n=0}^{N-1} p(n)(-1)^{\beta_2} = - \sum_{n=0}^{N-1} Q \sin(4\pi n/N)(-1)^{\beta_2} \quad (10)$$

As can be seen from Fig5, third order discrete WF with the normalized period of T has the discrete values defined as:

$$(-1)^{\beta_2} = \begin{cases} +1, & \text{at the intervals of } [0, N/4] \text{ and } [N/2, 3N/4] \\ -1, & \text{at the intervals of } [N/4, N/2] \text{ and } [3N/4, N-1] \end{cases}$$

So for the third-order component of the EP from (9) and (10) we obtain next equality

$$S(3) = \frac{1}{N} \sum_{n=0}^{N-1} P(n)(-1)^{\beta_2} \quad (11)$$

Considering (3) in the (12) we get

$$s(3) = \frac{1}{N} \sum_{n=0}^{N-1} \left(P - \left[P \cos\left(\frac{4\pi}{N} \cdot n\right) + Q \sin\left(\frac{4\pi}{N} \cdot n\right) \right] \right) (-1)^{\beta_2} \quad (12)$$

The next terms of this sum are equal to zero:

$$\frac{1}{N} \sum_{n=0}^{N-1} P(-1)^{\beta_2} = 0 \quad \text{and} \quad \frac{1}{N} \sum_{n=0}^{N-1} P \cos\left(\frac{4\pi}{N} \cdot n\right) (-1)^{\beta_2} = 0 \quad (13)$$

Considering these (13) becomes (See Fig.3):

$$S(3) = \frac{1}{N} \left[\sum_{n=0}^{N/4-1} Q \sin\left(\frac{4\pi}{N} n\right) - \sum_{n=N/4}^{N/2-1} Q \sin\left(\frac{4\pi}{N} n\right) + \sum_{n=N/2}^{3N/4-1} Q \sin\left(\frac{4\pi}{N} n\right) - \sum_{n=3N/4}^{N-1} Q \sin\left(\frac{4\pi}{N} n\right) \right] \quad (14)$$

The analysis indicated in Fig.3 intervals show that since the function of $\sin(4\pi n/N)$ has negative values at the intervals of $[N/4, N/2-1]$ and $[3N/4, N-1]$, then the Eq. (14) results in:

$$s(3) = \frac{1}{N} \sum_{n=0}^{N-1} Q \sin\left(\frac{4\pi}{N} n\right) \quad (15)$$

This expression defines the average value of the signal of

$$Q \sin\left(\frac{4\pi}{N} n\right)$$

and therefore is proportional to the average value of the RP in the investigated circuit.

V. ELECTRONIC REACTIVE POWER METER

Electronic RP meter's block diagram is shown in the Fig.6. The voltage and current signals are fed to the inputs of the analog multiplier(AD633), which produces time continuous output waveform which is proportional to the product of the input voltage and current signals, i.e. instantaneous power $p(t)$ defined by (1). Output waveform of AD633 is diagramed in the Fig.7a. The output of AD633 is fed to the analog-to-digital converter(ADC0804) controlled by the control logic(CL). The ADC0804 converts the input signal $p(t)$ to the output digital data samples $p(n)$ from each output signal of the digital sampler(DS). The digital samples $p(n)$ defined by (2) are shown in the Fig.7a. The sampling signals are formed from input voltage signal $u(t)$ to achieve the frequency insensitive measurement. The output signals of the DS are shown in the Fig.7b. The output from the ADC0804 is fed to the inputs of the up-down counter(UDC) through the multiplexer. The multiplexer is used to connect the output of the ADC0804 to either the up input or the down input of the UDC in accordance with the (14). First and third quarter parts of the $p(n)$, $i = 1,2,3,4,5,6,7,8,17,18,19,20,21,22,23,24$ (See Fig.8a) are entered to the up input and the second and fourth quarter parts of the $p(n)$, $i = 9,10,11,12,13,14,15,16,25,26,27,28,29,30,31,32$ (Fig.8b) are entered to the down input of the UDC. So in accordance with (14) the remainder number in the UDC to the end of the second period of the input signal becomes equal to the RP of the investigated circuit. The UDC binary output is indicated in the display.

VI. DIGITAL SAMPLER

The important component of the proposed electronic RP meter providing the independence of the measurement results from the change of input signal frequency is the DS. DS produces sampling signals with the predetermined frequency. Moreover,

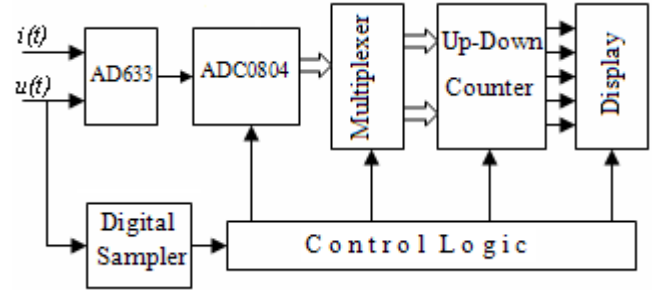


Fig.6. Block diagram of electronic powermeter

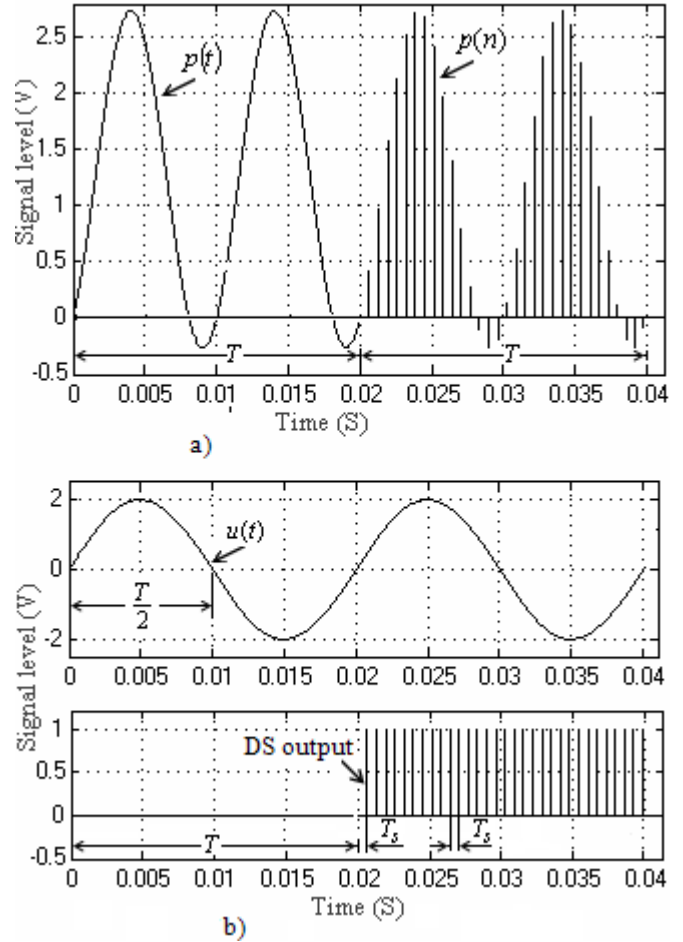


Fig.7. Output waveforms: a) analog multiplier and ADC; b) input $u(t)$ and DS output signals.

sampling frequency is correlated with the frequency of the input signal to be measured.

The block diagram of the DS is represented in the Fig.9. A zero crossing detector produces the pulses when input voltage signal $u(t)$ crosses the zero level. As seen from Fig.7b, the period of this impulses becomes the half($T/2$) of the full period T of the input voltage signal $u(t)$.

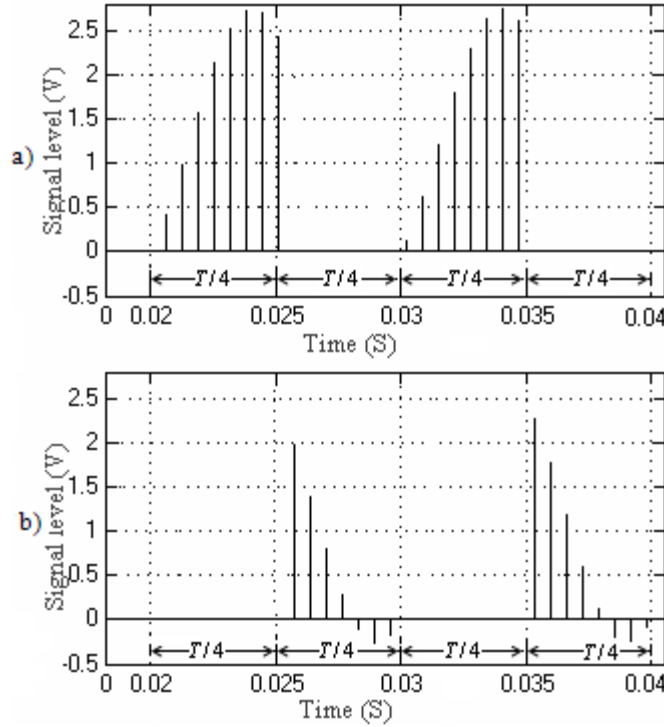


Fig.8. Sampled power signal $p(n)$: a) first and third quarter parts; b) second and fourth quarter parts.

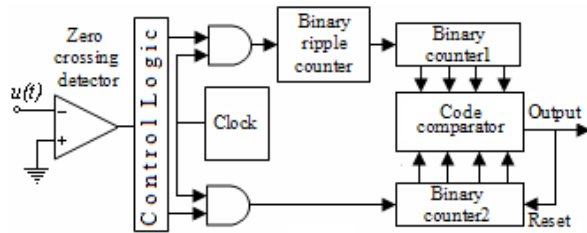


Fig.9. Digital sampler

During this first period of T the CL enables the output impulses of the clock to be passed through the binary ripple counter(BRC) only to the input of the binary storage counter1.

The counter capacity of the BRC is defined in accordance with the demand to the sampling rate of the instantaneous power signal $p(t)$.

The number of impulses stored in the binary storage counter1 to the end of time interval of T is given by

$$M = (f_s T) / N \quad (16)$$

Where, f_s is the clock frequency and N is the counter capacity of the BRC ($N = 2^m$, m is the number of bits). Note that, N is defined from Shannon criterion on sampling frequency At the beginning of the second

period T of $u(t)$ the CL enables the output impulses of the clock to be passed only to the input of the second binary storage counter2. When the number of the clock impulses stored in the second binary storage counter becomes equal to the M , i.e. the number, stored in the first BSC1 the code comparator(CC) produces its first output impulse. This impulse resets the BSC2 to zero and becomes the first output impulse of the DS(Fig.5b). Since the clock pulses continue to enter to the input of BSC2 continuously during second full period of T (Fig.5b). When the number of impulses counted by the BSC2 becomes again equal to the M , the CC produces the second output impulse of the DS resetting the BSC2 to zero.

The time interval between the instant of BSC2 was reset to zero and the time instant of BSC2 has counted M number of impulses is given by

$$T_s = f_c / M \quad (17)$$

Where T_s is the sampling interval(See Fig.5b) and $f_s = 1/T_s$ is the sampling frequency. Substitution (16) into (17) gives the expression relating sampling interval T_s to the input signal period T :

$$T_s = T / k \quad (18)$$

So repetition interval of the DS output impulses is the k times less the T . This relationship can also be written in terms of the DS input and output frequencies:

$$f_s = kf \quad (19)$$

It is evident from (18) and (19) that, the number of collected data N do not depend on the input signal frequency consequently, measurement results are also independent on the input signal frequency.

Carefully look at derived expressions of (18) and (19) allows to state that designed electronic meter meets the requirement of coherent data acquisition and thereby is the good solution for the preventing of the energy leaking from spectral components[16] when input signal frequency f is to vary because of the power distribution system instability. Thus, sampling period T_s becomes the function of the being sampled input signal period T . Proposed approach to DS implementation provides coherent data acquisition as a result avoids the spectral leakage in the comparatively wide range deviations of the power frequency in the investigated circuit. Thus, an extreme requirement on different algorithmic and hardware solutions to achieve the coherent sampling while dealing with the sampled data, is avoided.

IV. SIMULATION RESULTS

The simulation circuit of the proposed novel ASP structure for evaluation of RP and active power from instantaneous power $p(t)$ is shown in Fig.10. The simulation circuit includes: voltage source, $u(t)$; current source, $i(t)$; multiplier, which produces, the instantaneous power $p(t) = u(t)i(t)$; zero- and third-order Walsh code generators; the pair of multipliers for obtaining the products of the zero-and third-order WFs by $p(t)$; integrating analog-to-digital converters ADC1 and ADC2 used to produce digital codes proportional to the evaluated values of the active and the reactive components of the EP, respectively. During experimental studying the input voltage, $u(t)$ and the current, $i(t)$ signals were taken as [15,16]

$$u(t) = U_m \sin(\omega t) \text{ and } i(t) = I_m \sin(\omega t - \varphi) ,$$

where $I_m = 2A$, $U_m = 4V$, $\omega = 2\pi f$, $f = 50$ is the linear frequency in Hz, $\omega = 314$ is frequency in rad/sec, φ - phase

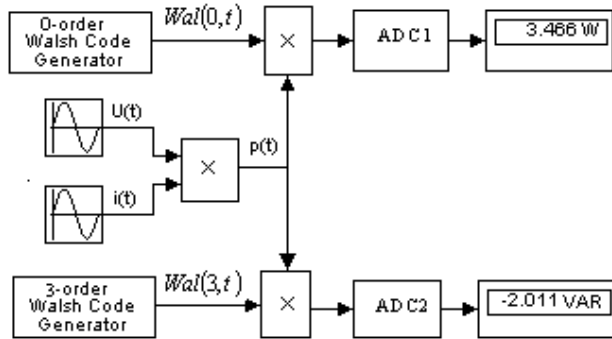


Fig.10. Proposed ASP technique based structure for the active and reactive power evaluation

shift between the voltage $u(t)$ and the current $i(t)$ signals. The phase shift, φ between the voltage $u(t)$ and the current $i(t)$ signals has been varied in the interval of $\varphi = 0 - 90^\circ$. The signal proportional to the instant value of the power $p(t)$ which is applied to the first inputs of the pair of multipliers is given by

$$p(t) = 8\sin(314t) * \sin(314t - \varphi)$$

The time representation of the signals $p(t)$ and $p(t) * Wa(3, \beta_k)$ are shown in the Fig.9. The signals $p(t)$ and $p(t) * Wa(3, \beta_k)$ are integrated and

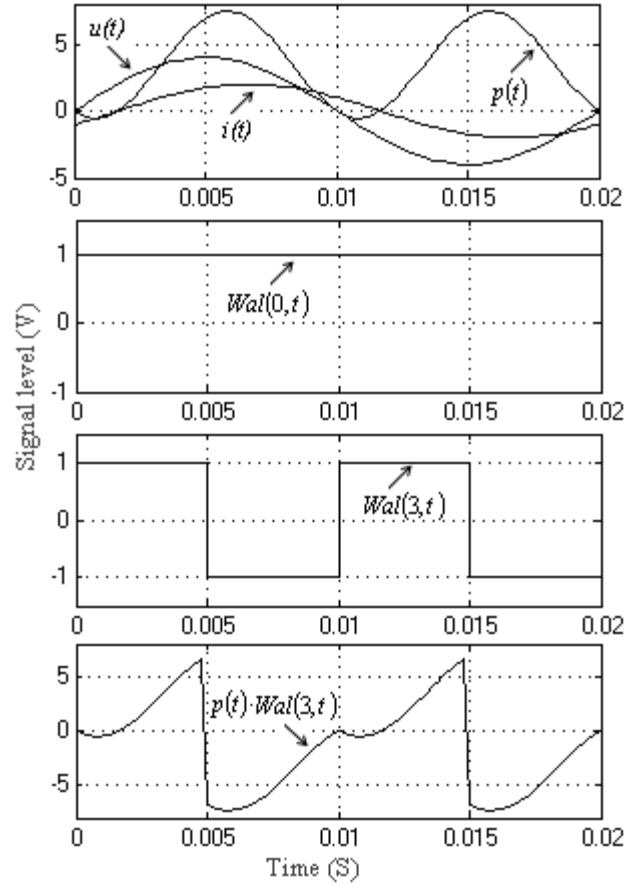


Fig.11. The Components outputs signals versus time representation

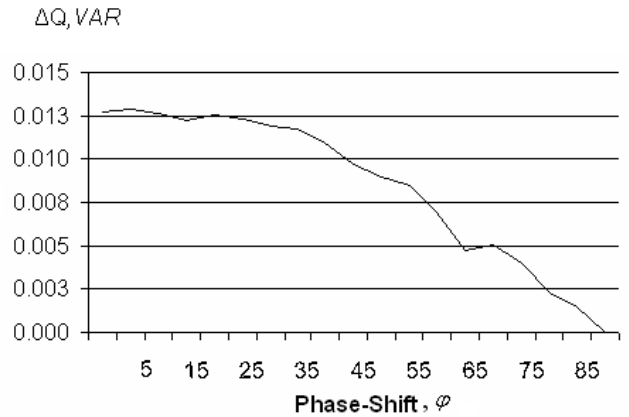


Fig.12. Relation between the measurement error ΔQ and the phase-shift rate φ .

converted to digital form using the ADC1 and ADC2, respectively. The digital codes, generated by ADC1 and ADC2 represent resulting evaluated values of the active and the reactive components of the electrical power (Fig.4). The results of the experimental verification are represented on the Table 1.

From the Fig.12 it can be seen the error appearing because of the change of the phase shift φ in the interval of from 0 to 90° .

The essential advantage of the proposed method for evaluation of RP has been verified by experimental studies. One of these advantages is that in contrast to the known existing methods the proposed method does not require a phase shift of the current signal to the $\pi/2$ with respect to the voltage signal.

The phase shift operation requires the corresponding hardware which may result in the additional measurement error.

The author is currently working towards the estimation and correction of harmonic distortions influence on proposed RP evaluation method.

VII. CONCLUSION

The evaluation of reactive component of EP with application of a WF simplifies the volume of computing operations on some order in comparison with sets of algorithms based on decomposition of signals on harmonics (trigonometric components). Evaluation of RP using WF results in certain advantages:

- during the processing of the signals on the base of WF time-shifting of the signals acts on the structure of the signals. This influence becomes useful during the evaluation of the power components allowing the obtaining extra knowledge concerning the phase-shifts on the harmonics of the input signals;
- the requirement of IEEE/IEC definition of a phase shift of $\pi/2$ between the voltage and the current signals, typical for reactive power evaluation, is eliminated from signal processing operation;
- the RP is evaluated without the phase-shift operation between the voltage and current waveforms to achieve increased efficiency of computational operations and hardware implementation;
- during DSP the multiplication of the sample values of the signals by corresponding order WF is performed simply, by alteration of sign of the signal samples from +1 to -1 only during even quarters of the input signal periods.

REFERENCES

- Fairney, W. "Reactive power-real or imaginary? ", *Power Engineering Journal*, Volume 8, Issue 2, April 1994, pp.69 – 75.
- W.-K. Yoon and M.J. Devaney. "Reactive Power Measurement Using the Wavelet Transform", *IEEE Trans. Instrum. Meas.*, vol. 49, pp 246-252, April 2000.
- Branislav Djokic, Eddy So, and Petar Bosnjakovic. "A High Performance Frequency Insensitive Quadrature Phase Shifter and Its Application in Reactive Power Measurements" *IEEE Trans. Instrum. Meas.*, vol. 49, pp 161-165, February 2000.

TABLE I
SIMULATION RESULTS OF THE RP EVALUATION
ALGORITHM.

	φ	Results of calculating		Outputs of the simulation circuit		Percentage error
		P,W	Q,VAR	P,W	Q,VAR	δ
0	0	4,000	0,000	4,002	-0,0127	100
1	5	3,985	-0,348	3,987	-0,3613	3,558
2	10	3,939	-0,694	3,941	-0,7069	1,790
3	15	3,864	-1,035	3,866	-1,047	1,169
4	20	3,759	-1,367	3,761	-1,38	0,912
5	25	3,626	-1,690	3,627	-1,702	0,724
6	30	3,465	-1,999	3,466	-2,011	0,593
7	35	3,277	-2,293	3,278	-2,305	0,508
8	40	3,065	-2,570	3,066	-2,581	0,424
9	45	2,830	-2,827	2,83	-2,837	0,342
10	50	2,573	-3,063	2,572	-3,072	0,292
11	55	2,296	-3,275	2,296	-3,284	0,259
12	60	2,002	-3,463	2,002	-3,47	0,201
13	65	1,693	-3,624	1,693	-3,629	0,131
14	70	1,370	-3,758	1,368	-3,763	0,135
15	75	1,038	-3,863	1,036	-3,867	0,103
16	80	0,697	-3,939	0,696	-3,941	0,057
17	85	0,352	-3,985	0,3469	-3,986	0,037
18	90	0,003	-4,000	0,0008	-4,0000	0,000

- S.L.Toral, J.M.Quero and L.G.Franquelo. "Reactive power and energy measurement in the frequency domain using random pulse arithmetic", *IEE Proc.-Sci. Technol.*, vol. 148, No. 2, pp.63-67, March 2001.
- Makram, E.B.; Haines, R.B.; Girgis, A.A. "Effect of harmonic distortion in reactive power measurement", *IEEE Trans. Industry Applications*, Volume 28, Issue 4, July-Aug. 1992, pp.782 – 787.
- T.W.S.Chow and Y.F.Yam. "Measurement and evaluation of instantaneous reactive power using neural networks", *IEEE Transactions on Power Delivery*, Vol. 9, No. 3, July 1994, pp.1253-1260.
- A. Ozdemir and A. Ferikoglu. "Low cost mixed-signal microcontroller based power measurement technique", *IEE Proc.-Sci. Meas. Technol.*, Vol. 151, No. 4, July 2004, pp.253-258.
- Soliman S.A., Alammari R.A., El-Hawary M.E., Mostafa M.A. "Effects of harmonic distortion on the active and reactive power measurements in the time domain: a single phase system" *Power Tech Proceedings, 2001 IEEE Porto*, Volume 1, 10-13 Sept. 2001, 6 pp.
- Emmanuel C. Ifeakor, Barrie W. Jervis. *Digital Signal Processing. A practical Approach*. Second Edition. Prentice Hall, 2002.
- Brandolini A., Gandelli A., Veroni F. "Energy meter testing based on Walsh transform algorithms", *Instrumentation and Measurement Technology Conference, 1994. Conference proceedings*, 10-12 May 1994, pp 1317 – 1320, vol.3.

11. Bai liyun, Wen biyang, Shen wei, and Wan xianrong. "Sample rate conversion using Walsh-transform for radar receiver", *Microwave Conference Proceedings*, 2005. APMC 2005. Asia-Pacific Conference Proceedings. Volume 1, 4-7 Dec. 2005, 4 pp.
12. M. Kezunovic, E. Soljanin, B. Perunicic, S. Levi, " New approach to the design of digital algorithms for electric power measurements", *IEEE Trans. on Power Delivery*, vol. 6, No 2, pp. 516–523, Apr. 1991.
13. Gonorovsky N.S. *Radio Engineering Circuits and Signals: Studies*. - M.: Sov. Radio, 1977. -608 p
14. Trachtman A.M., Trachtman V.A. *Fundamentals of the discrete signals' theory on the finite intervals*. - M.: Sov. Radio, 1975. -208 p.
15. Abiyev A.N., Aliyev I.M. An Electric Power Measurement Based On Discrete Walsh Transformation.// Proceedings of the International Conference *Interactive Systems: The Problems Of Human-Computer Interaction*, 23-27 September 2003, Ulyanovsk, Russia, pp.195-196.
16. Adalet N. Abiyev, "The Walsh Function Based Electric Power Measuring Method", Proceedings of the *3rd International Symposium on Electrical, Electronics, and Computer Engineering*, November 23-25, 2006. Nicosia, North Cyprus, pp.177-181.
17. P. Carbone and D. Petri, "Average power estimation under nonsinusoidal conditions", *IEEE Trans. Instrum. Meas.*, vol. 49, No 2, pp. 333–336, Apr. 2000.